J Mater Sci (2009) 44:897–902
DOI 10.1007/s10853-008-3001-7

Microstructural study of adiabatic shear bands formed in serrated chips during high-speed machining of hardened steel

C. Z. Duan · Y. J. Cai · M. J. Wang · G. H. Li

Received: 18 December 2007 / Accepted: 11 September 2008 / Published online: 13 January 2009

Abstract The characterization of the microstructure and phase transformation in adiabatic shear bands (ASB_s) within the serrated chips generated during high-speed machining of hardened $30CrNi_3MoV$ steel has been performed. The observations showed that the microstructure gradually changes from the center of the ASB to the matrix of the chip, the fine equiaxed grains appear with size of about 0.4–0.6 μm in the center of the ASB_s, the transitional region adjacent to the ASB is characterized by the broken and elongated martensite laths in shear direction. The analysis indicated that the serrated chip formation was likely due to adiabatic shear instability that occurred in the primary shear zones and the transformation to martensite within the ASB. Dynamic recovery and recrystallization are the dominant metallurgical processes during microstructural evolution of ASB.

Introduction

Adiabatic shear band (ASB) formation is a special metallurgical phenomena observed in a variety of materials which are subjected to high strain rate deformation such as ballistic impact, explosive fragmentation, high energy rate forming, etc. ASBs form as a result of the equilibrium between strain hardening and thermal-softening during adiabatic deformation. The shear deformation of the material is highly localized in very narrow ASBs. In the past 20 years, the formation and microstructural evolution of ASBs have received much attention as evidenced by the significant number of papers describing the phenomena by Rogers [1], Wittman et al. [2], Meyers [3–6], Cho [7], Bai [8], Xu [9], etc.

As a result of the high-speed machining process, which involves large strains, high strain rates, and heat localization, ASB_s have been frequently observed in the primary shear zones within the serrated chips of some difficult-to-machine materials [10–12]. Characterization of the ASB microstructure generated during high-speed machining of difficult-to-machine materials is very important for understanding the formation mechanisms of serrated chip and for the numerical simulation of chip formation in addition to the optimization of high-speed machining process. However, there has been little work reported concerning the formation and microstructure of these ASBs due to the difficulty of specimen preparation, particularly for transmission electron microscopy (TEM) samples. This paper presents the results of the microstructural characterization of ASB_s in the serrated chips produced during high-speed orthogonal cutting of hardened $30CrNi_3MoV$ structural steel. The phase transformation and evolution of the microstructure in the ASB are discussed.

Experimental procedure

Material and cutting tests

$30CrNi_3MoV$ high strength low alloy steel with composition (in wt.%) of 0.30% C, 0.90% Cr, 3.15% Ni, 0.30%

C. Z. Duan (✉) · M. J. Wang · G. H. Li
Key Laboratory of Ministry of Education for Precision and Non-traditional Machining, School of Mechanical Engineering, Dalian University of Technology, Dalian 116023, China
e-mail: dcz71@163.com

C. Z. Duan · Y. J. Cai
Tianjin Key Laboratory of High Speed Cutting & Precision Machining, Tianjin University of Technology and Education, Tianjin 300222, China

Mo, 0.20% V, 0.27% Si, 0.45% Mn, and balance Fe, was selected for the present study. The experimental materials were machined into disc specimens, 95 mm in diameter and 3.5 mm in height. The specimens were quenched from 890 °C and then tempered at 200 °C for 2 h, with a final hardness of 48HRC. The orthogonal cutting tests were performed on a high-speed lathe with cutting speed of 300 m min^{-1}, the cutting thickness of 0.215 mm, the cutting width of 3.5 mm, and the tool rake angle of −10°. The cutting forces F_C and F_T were measured by a dynamometer during the cutting test operation.

Metallurgical sample preparation

The serrated chips were collected and were subsequently evaluated using light optical microscopy, microhardness testing, scanning electron microscopy (SEM), and X-ray diffractometry (XRD). The chips were mounted and polished using conventional metallographic procedures. The height of the chips and sawtooths, the separation angles between shear band and bottom of chip, and the shear band width were measured. The microstructure of the chip and the ASB_s were analyzed using TEM. Suitable thin-foil specimens for TEM characterization were prepared by electroplating metal on to two sides of the chips to increase the total area prior to electropolishing.

Results and discussion

ASB microstructure

Figure 1 is a schematic of serrated chip formation during high-speed orthogonal cutting. Localized shear deformation occurred in the primary shear zone of the chip during cutting leading to serrated chip. The repeated ASB_s with large levels of deformation were formed between the sawtooths. Figure 2 is a light optical micrograph of a

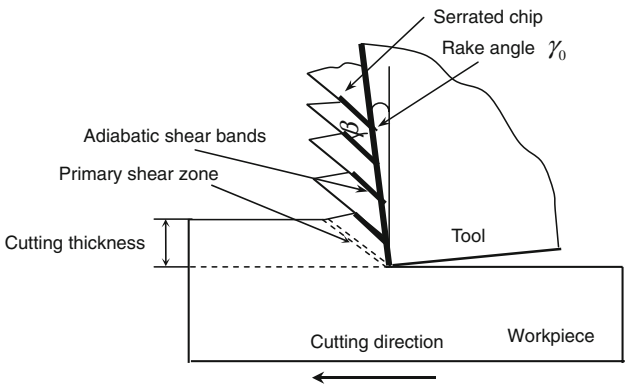

Fig. 1 Schematic of serrated chip formation during high-speed orthogonal cutting

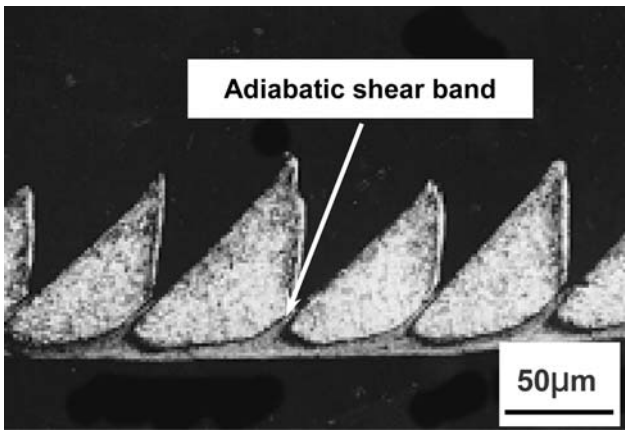

Fig. 2 A serrated chip with ASB_s

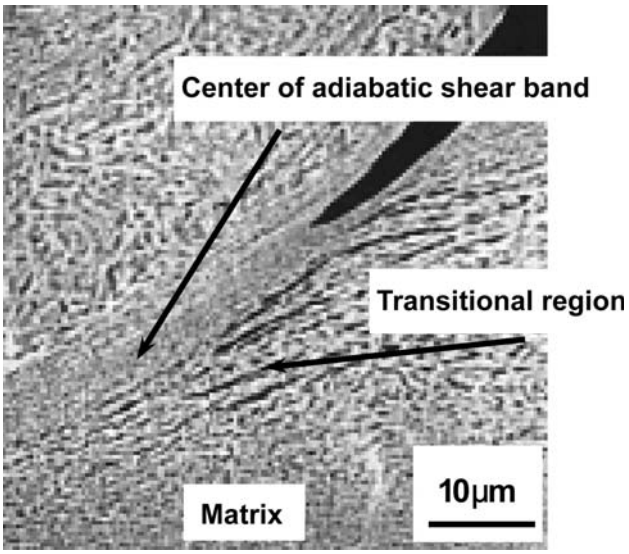

Fig. 3 A SEM micrograph of the primary deformation zone

serrated chip produced during high-speed machining $30CrNi_3MoV$. It can be seen that the ASB_s are periodically aligned along the primary shear zones, and the deformation is localized within the ASB_s. The ASB_s, which are about 10 μm in width, appear significantly different from the matrix of the chip.

Figure 3 is a SEM image of an ASB which contains distinct boundaries and has a well-defined width. It does not show any pronounced deformation features in the center of the ASB. The microstructure gradually changes from the center of the ASB to the matrix of the chip. Fine grains are present in the center of the ASB. In the transitional regions near the shear band center the microstructure is elongated along the shear band direction. In Fig. 3, several features can be observed. Firstly, the absence of any cracks or voids within or near the shear bands seems to indicate that serrated chip formation does not occur by a crack initiation and growth mechanism. Secondly, the

thickness of the ASB is not uniform, but gradually increases from the root of the sawtooth to the bottom of the chip suggesting shear strain undulation. In addition, the microstructure inside the ASB is considerably different from that outside the ASB. The fine grains, which do not appear to exhibit evidence of deformation, are observed in the center of the ASB, but the severely deformed and damaged structures are clearly evident in the transitional regions between the center of the shear band and the matrix of the chip. The results of Fig. 3 indicate that the serrated chip formation may be due to adiabatic shear instability occurring in the primary shear zones, during which the adiabatic deformation localization and grain refinement were generated in the primary shear zones.

Phase transformation within ASB

Microhardness measurements transverse to the ASB are shown in the microhardness profile of Fig. 4. It is seen clearly that the microhardness values in and near the ASB decrease with distance from the center of ASB until the matrix hardness is reached, and that the hardness in the center of the ASB is higher than that of the martensite.

X-ray diffraction was used to assess the possible occurrence of a non-diffusional phase transformation in the ASB_s. Figure 5 shows X-ray diffraction spectra before and after high-speed machining. It was confirmed that the uncut sample contains only the body-centered cubic α phase and some carbides, but the ASB in the machined chip was a mixture of α phase and face-centered cubic γ phase together with carbides because the (111) and (220) diffraction peaks of γ phase appear. This indicates that α phase was transformed to γ phase due to the high temperature generated during the high-speed machining. In turn, γ phase was quenched to martensite in the form of non-diffusional phase transformation. The austenization temperature of $30CrNi_3MoV$ steel is about 750 °C; therefore, the result of this study implies that the temperature within the ASB reaches at least 750 °C.

Microstructure of ASB

The microstructure of different regions in or near the ASB was characterized by TEM as shown in Figs. 6–8. Figure 6a shows the lath structure in the matrix, located away from the center of ASB, which was characterized by a relatively homogeneous distribution of dislocations and carbides. The electron diffraction pattern in Fig. 6b is consistent with the martensite. The transitional region adjacent to the shear band was characterized by somewhat finer martensite laths in the shear direction as shown in Fig. 7a. The spots are slightly elongated in Fig. 7b, which means that the material was subjected to large deformation, but its crystallography structure is retained.

The deformation twins and martensite laths cannot be seen at the center of the ASB as shown in Fig. 8a. The microstructure in the central region of the shear band consists of very fine equiaxed grains with size of about 0.4–0.6 μm and very low density of dislocations. These equiaxed grains with high-angle misorientation are similar to dynamic recrystallization microstructure, but their size is much

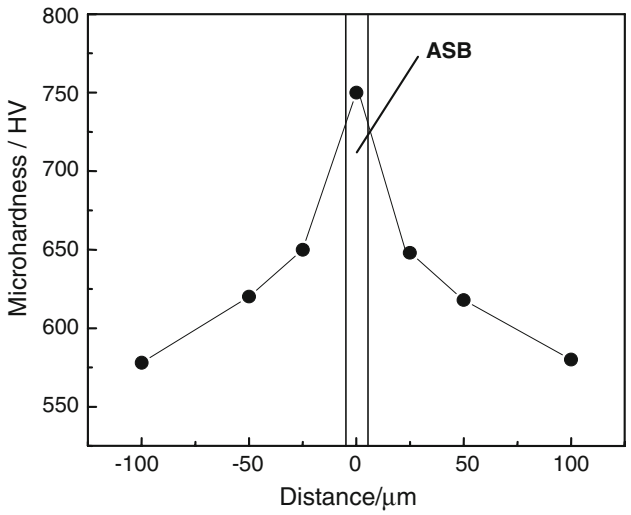

Fig. 4 Distribution of microhardness across ASB

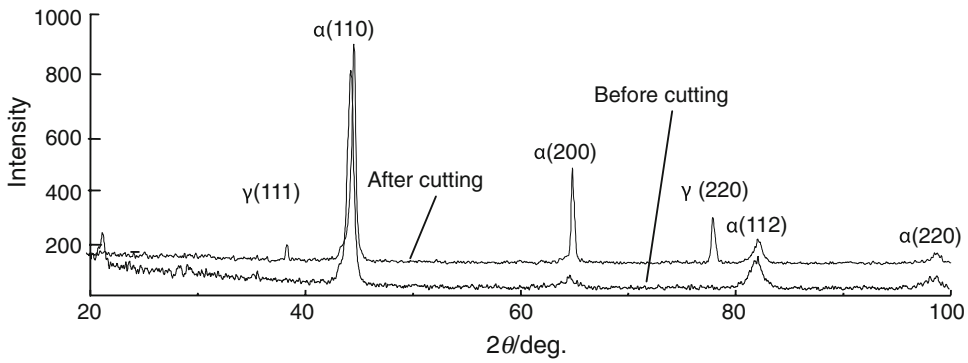

Fig. 5 X-ray diffraction peaks of the ASB in the serrated chip in comparison with uncutted sample

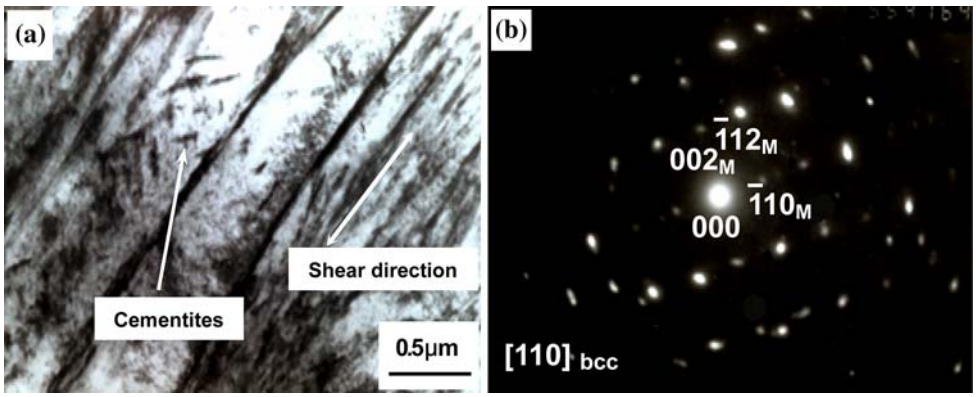

Fig. 6 TEM micrographs of the serrated chip matrix **a** maretnsite lath structure (BF image), **b** diffraction pattern

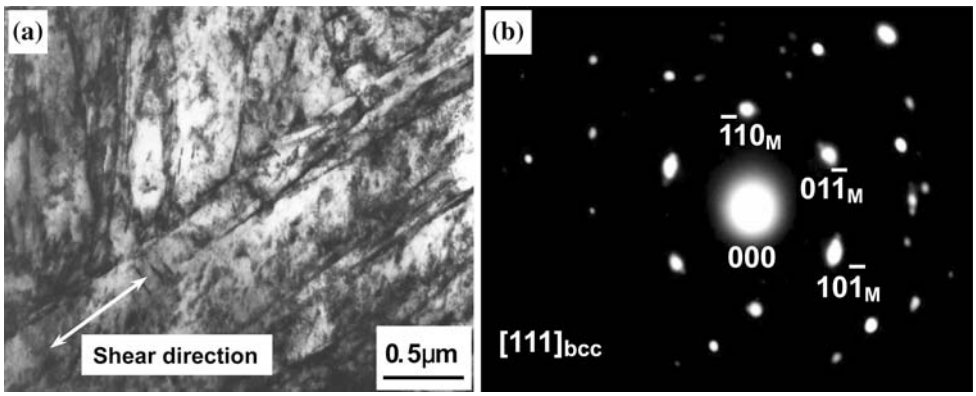

Fig. 7 TEM micrographs of the transitional region near the ASB **a** elongated and broken martensite laths along shear direction, **b** corresponding diffraction pattern

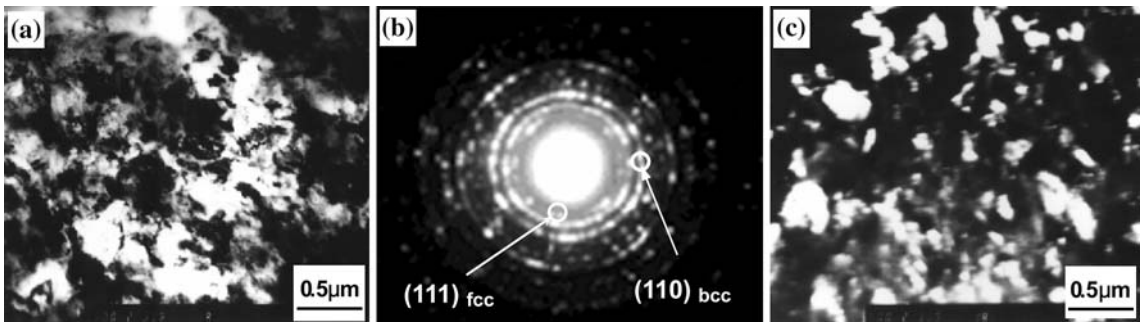

Fig. 8 TEM micrographs of the center in the ASB **a** dynamic recrystallization microstructure (BF image), **b** diffraction pattern, **c** DF image from the $(110)_{bcc}$ martensite reflection

smaller than that of conventional recrystallization grains. In addition, some ultra-fine carbide particles are observed between the equiaxed grains. The diffraction patterns arising from the shear band show that there is a nearly continuous ring of orientations on which there are distributed discontinuous spots as shown in Fig. 8b. A dark field image from the shear band more clearly reveals the equiaxed grains in the shear band center as shown in Fig. 8c. These results are similar to those obtained under high strain rate loading condition recently by Meyers et al. [6], Xu et al. [9].

Based on the present observations, it is suggested that dynamic recovery and recrystallization are the dominant metallurgical processes during microstructure evolution of ASB. A schematic diagram of the microstructure evolution model is presented in Fig. 9a–d. When tempered martensite (Fig. 9a) is deformed at high dynamic strain rates, the severe plastic flow induces reorientation and elongation of the martensite laths in the shear direction, as shown in Figs. 6a and 9b. A dynamic recovery process begins, in which dislocations begin to arrange in cell boundaries. This process is enhanced by a simultaneous increase in local temperature as the deformation localizes. Aided by the local increase in temperature, dislocations move and condense into tangles, producing regions of high and low dislocation density and forming clearly defined subgrain boundaries; these elongated grains are often partitioned by transverse cell walls of

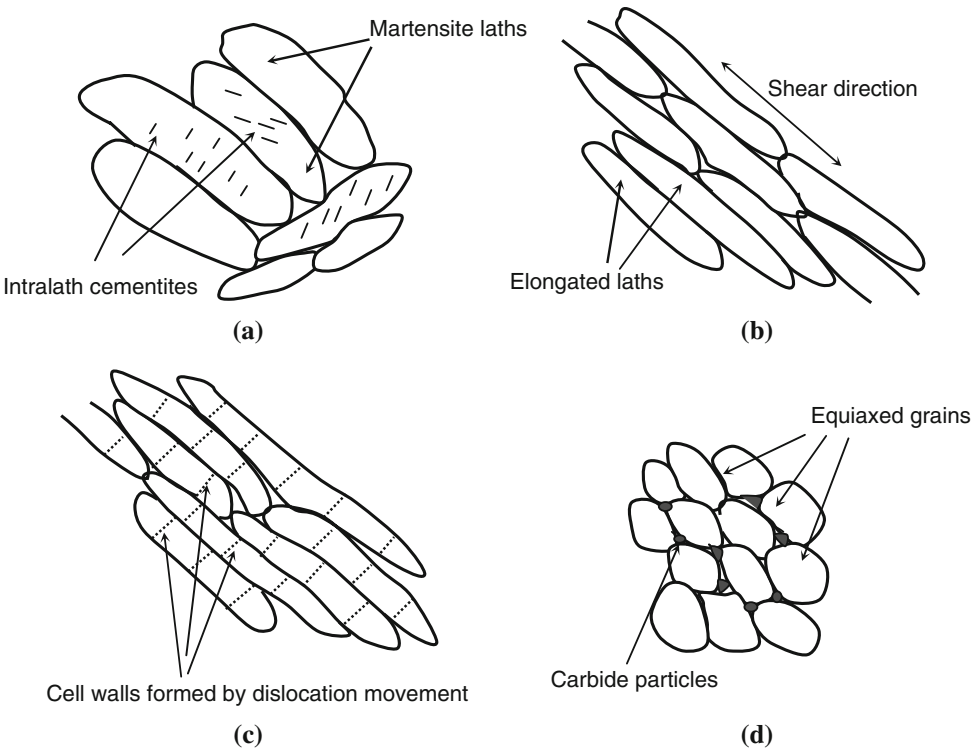

Fig. 9 Schematic diagram of microcosmic model of microstructure evolution during formation of ASB **a** tempered martensite, **b** martensite laths in shear direction, **c** partitioning of elongation subgrains into rectangular cells, **d** formation of equiaxed structure

variable widths, as shown in Figs. 7a and 9c. Finally, these fine subgrains are transformed into the equiaxed grains aided by adiabatic temperature and shear stress; it is a dynamic recrystallization process, as shown in Figs. 8 and 9d. The similar microstructure evolution was observed in dynamic torsional deformation of steel [7].

The occurrence of the equiaxed grains in the ASB can be explained by a rotational recrystallization mechanism under high strain rate loading which was proposed by Meyers and Pak [4]. The deformation time during high-speed cutting is very short; hence, it is unlikely that the grains of 0.6 μm size were formed by migration of the grain boundaries. Thus, conventional recrystallization appears unlikely. A series of microstructural changes during a rotational recrystallization were described in details by Meyers et al. [3]. Since the dynamic recrystallization process during ASB formation is not explained by migration of the grain boundaries, the size of the equiaxed grains within the ASB_s of the serrated chips cannot be calculated using the recrystallization dynamic equations controlled by atomic thermal migration. Derby [13] proposed that the recrystallization grain size produced by subgrain rotation is directly proportional to the applied stress value by:

$$\frac{\sigma\delta}{\mu b} = K \tag{1}$$

where σ is the applied stress, δ is the recrystallization grain size, μ is the elastic shear modulus, b is the Burgers vector magnitude, κ is the material constant, $\kappa \approx 10$ for metals. Under the orthogonal cutting condition, the applied stress σ is the average shear stress τ in primary shear zone.

For $30CrNi_3MoV$ steel in this investigation, at the cutting speed of 300 m min^{-1}, the average shear stress τ can be calculated using Eq. 2.

$$\tau = \frac{\sin\beta[F_C\sin(\beta-\gamma_0) - F_T\cos(\beta-\gamma_0)]}{(H-\frac{h}{2})a_w} \tag{2}$$

where F_C and F_T are the cutting forces, β is the included angle between the shear band and bottom of the chip, γ_0 is the tool rake angle, H is the height of the chip, h is the height of the sawtooth, a_w is the cutting width. All parameters are known or can be obtained by measuring.

For α-Fe, the magnitude of the Burgers vector $b = 2.48 \times 10^{-10}$, and the elastic shear modulus $\mu = 83$ GPa. From Eq. 2, the calculated recrystallization grain size in the ASB 0.6 μm is consistent with the observations in Fig. 9. Thus, one may conclude that the dynamic recrystallization by a rotational mechanism takes places in ASB_s, it is leading reason of material softening in primary shear zone inducing serrated chip formation.

Conclusions

Based on the microstructural observation and analysis of the ASB within the serrated chips generated during the high-speed machining of hardened $30CrNi_3MoV$ steel, the following can be concluded:

(1) The ASB_s with widths of about 10 μm are significantly different from the matrix of the chip. The microstructure gradually changes from the center of the ASB to the matrix of the chip. The serrated chip formation should be due to adiabatic shear instability occurring in the primary shear zones, during which the adiabatic deformation localization and grain refining were generated in the primary shear zones.
(2) The microhardness in the center of the ASB is higher than that of martensite in the chip.
(3) The fine equiaxed grains approximately 0.4–0.6 μm in size were formed in the center of the ASB_s, whereas the transitional region adjacent to the ASB was characterized by martensite laths, some of which appeared elongated in the shear direction. The microstructural evolution of dynamic recovery and recrystallization is the dominant metallurgical process during microstructural evolution of ASB. The formation of the equiaxed grain size in the center of the ASB can be better explained using theory of rotational dynamic recrystallization under high strain rate loading.

Acknowledgements This research is supported by National Natural Science Foundation(50875033, 50775018), by the Natural Science Key Foundation of Tianjin (No.08JCZDJC18400),and by Tianjin Key Laboratory of High Speed Cutting & Precision Machining. The authors are grateful to Prof. Xu Yongbo for his contribution in the microscopic analysis.

References

1. Rogers HC (1979) Annu Rev Mater Sci 9:283. doi:10.1146/annurev.ms.09.080179.001435
2. Wittman CL, Meyers MA, Pak HR (1990) Metall Trans 21A:707
3. Meyers MA, Wittman CL (1990) Metall Trans 21A:3153
4. Meyers MA, Pak HR (1986) Acta Metall 34:2493. doi:10.1016/0001-6160(86)90152-5
5. Meyers MA, Andrade UR, Chokshi AH (1995) Metall Trans 26A:2881
6. Meyers MA, Nesterenko VF, LaSalvia JC et al (2001) Mater Sci Eng A 317:204. doi:10.1016/S0921-5093(01)01160-1
7. Cho K, Lee S, Nutt SR et al (1993) Acta Metall Mater 41:923. doi:10.1016/0956-7151(93)90026-O
8. Bai YL, Xue Q, Xu YB et al (1994) Acta Metall Mater 17:155
9. Xu YB, Ling Z, Wu X et al (2002) J Mater Sci Technol 18:504
10. Xie JQ, Bayoumi AE, Zbib HM (1996) Int J Mach Tools Manuf 7:835. doi:10.1016/0890-6955(95)00016-X
11. Molinari A, Musquar C, Sutter G (2002) Int J Plast 18:443. doi:10.1016/S0749-6419(01)00003-1
12. Campbell CE, Bendersky LA, Boettinger WJ et al (2007) Mater Sci Eng A 430:15. doi:10.1016/j.msea.2006.04.122
13. Derby B (1991) Acta Metall Mater 39:955. doi:10.1016/0956-7151(91)90295-C